Published in final edited form as:
Epilepsia. 2017 May 01; 58(5): 858–871. doi:10.1111/epi.13719.

$Ca_v1.3$ channels play a crucial role in the formation of paroxysmal depolarization shifts in cultured hippocampal neurons

Victoria Stiglbauer, **Matej Hotka**, **Manuel Ruiß**, **Karlheinz Hilber**, **Stefan Boehm**, **Helmut Kubista**
Department of Neurophysiology and -pharmacology, Center of Physiology and Pharmacology, Medical University of Vienna, 1090 Vienna, Austria

Summary

Objective—An increase of neuronal $Ca_v1.3$ L-type calcium channels (LTCCs) has been observed in various animal models of epilepsy. However, LTCC inhibitors failed in clinical trials of epileptic treatment. There is compelling evidence that paroxysmal depolarization shifts (PDS) involve Ca^{2+}-influx through LTCCs. PDS represent a hallmark of epileptiform activity. In recent years, a probable epileptogenic role of PDS has been proposed. However, the implication of the two neuronal LTCC isoforms, $Ca_v1.2$ and $Ca_v1.3$, in PDS remained unknown. Moreover, Ca^{2+}-dependent nonspecific cation (CAN) channels have also been suspected to contribute to PDS. Nevertheless, direct experimental support of an important role of CAN channel activation in PDS formation is still lacking.

Methods—Primary neuronal networks derived from dissociated hippocampal neurons were generated from mice expressing either a dihydropyridine-insensitive $Ca_v1.2$ mutant ($Ca_v1.2DHP^{-/-}$ mice) or from $Ca_v1.3^{-/-}$ knockout mice. To investigate the role of $Ca_v1.2$ and $Ca_v1.3$, perforated patch-clamp recordings were made of epileptiform activity which was elicited using either bicuculline or caffeine. LTCC activity was modulated using the dihydropyridines Bay K 8644 (agonist) and isradipine (antagonist).

Results—Distinct PDS could be elicited upon LTCC potentiation in $Ca_v1.2DHP^{-/-}$ neurons but not in $Ca_v1.3^{-/-}$ neurons. In contrast, when bicuculline led to long-lasting, seizure-like discharge events rather than PDS, these were prolonged in $Ca_v1.3^{-/-}$ neurons but not in $Ca_v1.2DHP^{-/-}$ neurons. Since only the $Ca_v1.2$ isoform is functionally coupled to CAN channels in primary hippocampal networks, PDS formation does not require CAN channel activity.

Significance—Our data suggest that the LTCC requirement of PDS relates primarily to $Ca_v1.3$ channels rather than to $Ca_v1.2$ channels and CAN channels in hippocampal neurons. Hence,

Correspondence to: Helmut Kubista.

Author for correspondence: Assoc.-Prof. Helmut Kubista, PhD, Center of Physiology and Pharmacology, Department of Neurophysiology and -pharmacology, Medical University of Vienna, Waehringerstrasse 13a, 1090 Vienna, Austria, Phone: +43 1 40160 31240; Fax: +43 1 40160 931300, helmut.kubista@meduniwien.ac.at.

Disclosure

None of the authors has any conflict of interest to disclose. We confirm that we have read the Journal's position on issues involved in ethical publication and affirm that this report is consistent with those guidelines.

Europe PMC Funders Author Manuscripts

$Ca_v1.3$ may represent a new therapeutic target for suppression of PDS development. The proposed epileptogenic role of PDS may allow for a prophylactic rather than the unsuccessful seizure suppressing application of LTCC inhibitors.

Keywords

L-type voltage-gated calcium channels; CAN channels; epileptogenesis; primary cultured hippocampal neurons

Introduction

L-type voltage gated calcium channels (LTCCs) are localized preferentially to the somatodendritic area of neurons and play a crucial role in the regulation of neuronal excitability[1]. Ca^{2+}-inward currents via LTCC directly depolarize neuronal membranes and this gives rise to electrophysiological phenomena such as burst discharges, upstates and plateau potentials[1, 2, 3]. In line with such a role in central neurons, anti-epileptic effects have been described for nimodipine and other dihydropyridine (DHP)-type LTCC inhibitors in experimental studies, but a lack of effect has also been reported repeatedly (reviewed in[4]). Importantly, nimodipine (a brain permeant DHP) failed in clinical trials of epileptic treatment[4]. Although concerns have been raised regarding the validity of these studies (for example regarding the inclusion of patients with very refractory seizure disorders or the relatively low serum concentrations of dihydropyridines that were reached as a result of pharmacokinetic interactions with concurrently applied antiepileptic drugs)[4], dihydropyridines are not considered to represent valuable anti-epileptic therapeutic options.

These findings are in stark contrast with accumulating evidence of a prominent role of $Ca_v1.3$ in epilepsy. In hippocampal neurons of spontaneously epileptic rats (SER), Ca^{2+}-influx through LTCCs was much greater than in those of normal animals[5]. Current-voltage curves revealed a pronounced increase of the calcium current, especially at the more hyperpolarized voltages[6], in a region where activation of $Ca_v1.3$ rather than $Ca_v1.2$ is believed to predominate[7]. Indeed, elevated levels of $Ca_v1.3$ (but not of $Ca_v1.2$) were reported in neurons of epileptic Wistar Albino Glaxo rats from Rijswijk (WAG/Rij), of the genetically epilepsy prone rat (GEPR) and of the seizure-prone gerbil[8, 9, 10]. Moreover, CACNA1D (coding for $Ca_v1.3$) - but not CACNA1C (coding for $Ca_v1.2$) - has been identified as a risk gene in human epilepsy[11], and considerations regarding the nature and the site of mutations in CACNA1D suggested a gain-of function of $Ca_v1.3$ channels[12].

A particular epileptiform discharge event for which a crucial contribution of LTCCs has been identified[13, 14, 15, 16, 17] is the so-called paroxysmal depolarization shift (PDS)[18]. In its broadest sense, the PDS represents a “burst pattern of discharge generated by an abnormal depolarization of neuronal membranes”[19]. It has been viewed in this respect as the hallmark of epileptic discharge[20]. However, PDS were originally described *in vivo* in brain tissue challenged with $GABA_A$ receptor antagonistic concentrations of penicillin[18]. They were identified as the single neuron correlate (recorded with an intracellular electrode) of electrographic spikes that can be detected simultaneously at the brain cortex (with a cortical surface electrode), notably prior to epileptic seizures. The typical voltage trajectories of

Europe PMC Funders Author Manuscripts

these PDS were described as positive shifts of membrane voltage “up to 30 mV or occasionally more” with “durations from 40 up to 400 ms or more”, during which “spike generation would progressively decrease in amplitude until only small oscillations remained riding on top of the PDS”[18]. In this respect, PDS closely resembled giant depolarizing potentials (GDPs), brief discharges that govern self-organization of developing brain circuits[21]. It should be noted that a close resemblance to GDPs only applies to the original type of PDS, which cannot be triggered by current injections into neuronal somata and were suggested to arise from synaptic activity in the dendritic compartment[16, 22]. This feature distinguishes original PDS (to which we refer to in our study) from various other kinds of PDS-like electrical events, such as persistent sodium current-dependent burst discharges[23, 24]. The resemblance to GDPS, together with the finding that electrographic spikes appear immediately after injury in human and experimental epilepsy[25], e.g. during the silent epileptogenic period of status epilepticus-induced animal models of acquired epilepsy ([26] and citations therein), support the idea that PDS may play a role in the processes leading to epilepsy[25, 27]. Since LTCCs play an essential role in the formation of these putatively epileptogenic events[17], the implication of $Ca_v1.3$ increases in epilepsy may also rely on an involvement in PDS formation. Hence, considering the proposed role of PDS in epileptogenesis, $Ca_v1.3$ may be involved in the processes leading to epilepsy rather than in actual seizure activity. This would change the view of how LTCC inhibitors could be beneficially used in epileptic therapy. However, Ca^{2+}-dependent unspecific cation (CAN) channels have also been proposed to contribute to PDS[28]. Hence, the role of direct Ca^{2+}-influx via LTCCs as opposed to LTCC-mediated CAN channel currents in PDS remained unclear (Fig. 1).

Various genetically modified mouse models are meanwhile available to study the physiological and pathophysiological role of LTCC isoforms. We have recently employed two models to investigate the implication of the two neuronal LTCCs, viz. $Ca_v1.2$ and $Ca_v1.3$ channels, in neuronal excitability[29]. One is a classical knockout of $Ca_v1.3$ channels ($Ca_v1.3^{-/-}$ mice, see [30]), the other one, $Ca_v1.2DHP^{-/-}$, a “pharmacological knockout”, where the gene encoding for $Ca_v1.2$ channel protein was exchanged for one which leads to expression of a mutant version that displays reduced sensitivity to dihydropyridines (see [31]). These mouse models were used in this study to investigate the role of $Ca_v1.3$ and $Ca_v1.2$ in PDS formation.

Methods

Mouse models

The origin and keeping of $Ca_v1.3^{-/-}$ [30] and $Ca_v1.2DHP^{-/-}$ mice[31] was as described elsewhere[29]. Genotypes were confirmed by conventional PCR testing of DNA extracted from the mouse tails. All experiments were performed *ex-vivo*. Animal care and use conformed to institutional policies and guidelines. In addition, the use of genetically modified mice was approved according to the Austrian animal protection act under the reference number BMWFW-66.009/0316-WF/V3b/2014.

Rationale of using primary neuronal networks

Experiments were performed on neuronal networks that develop from dissociated hippocampal neurons in co-culture with glial cells. The primary culture allowed us to use the neurons for experiments after they have had sufficient time to recover from acute stress of the isolation procedure, which may otherwise hinder the controlled induction of a defined type of PDS. Moreover, we have obtained broad experience with this preparation from our previous work, in particular regarding LTCC-CAN channel coupling[17, 29, 32]. A similar experimental system has been widely used in basic research on acquired forms of epilepsy ([33] and citations therein). Low-Mg^{2+}- induced seizure-like activity in our cultured hippocampal networks displayed the characteristic pattern (e.g. tonic-like period followed by clonic-like afterdischarges, see [34]) described previously by other authors in hippocampal brain slices. The use of primary hippocampal networks allowed us to fully comply with recommendations of the ARRIVE and Basel declaration (http://www.basel.declaration.org), as requested by the journal's guidelines. PDS may not depend on complex neuronal network circuitry, since they have been recorded in microisland cultures consisting of only a few neurons, or even single neurons with autapses[35, 36]. PDS are believed to be caused by an interplay of synaptic hyperactivity and abnormal endogenous conductances[37, 38]. In line with this notion, PDS could be prevented by inhibition of fast glutamatergic neurotransmission (e.g. using CNQX (6-cyano-7-nitroquinoxaline-2,3-dione), [Fig. S3D]), and were largely reduced by blockage of LTCCs ([17] and unpublished data using bicuculline for induction of PDS [Fig. S3A-S3C]), which provide a major somatodendritic ion conductance[39]. The dual dependence of PDS on excitatory neurotransmission and LTCCs has been confirmed in *in vivo* recordings and in experiments on brain slices[13, 40, 41]. The wide similarities argue against fundamental differences between PDS recoded *in vitro* and *in vivo*. Hence, considering the 3R concept outlined in the Basel declaration, the use of primary neuronal networks thus appears indicated, in particular at this stage of target identification. One mouse pup usually suffices to generate neuronal culture dishes for at least 8 days of experimentation (details of the preparation are given below), which allowed us to considerably reduce the number of animals needed to sacrifice. Moreover, neonatal mice were preferred rather than embryos, because the latter would have necessitated the killing of a gestating animal.

Generation of primary neuronal networks

The generation and maintenance of neuron/glia co-cultures, including culture media, as well as electrophysiological characteristics were described in detail previously[17, 32]. In brief, hippocampi were excised from decapitated new born mouse pups (i.e. within 24 hours after birth). After dissociation of cells from the papain-treated hippocampi, 50 000 cells were seeded with the help of glass rings onto about 40 mm^2 circle areas in the middle of a 3 cm diameter poly-D-lysine-coated culture dish containing medium supplemented with antibiotics (penicillin/streptomycin, see [32] for details). The glass rings were removed after 2 hours. Non-attached cells were removed after 18 to 24 hours by exchange of the medium with the same one but containing no antibiotics. After three days, glial cell division was stopped by addition of 1 μM cytosine arabinoside. Neurons were then allowed to form neuronal networks for at least nine days on the glial cell layer. Neuronal networks were used for experiments after a total of 12 to 20 days in culture [Fig. S1].

Electrophysiology

Electrophysiological experiments were performed at room temperature using the perforated-patch clamp technique with a Multiclamp 700B amplifier (Axon Instruments), a Digidata 1440A digitizer (Molecular Devices, Sunnyvale, CA, USA) and the pCLAMP 10.2 electrophysiology data acquisition (Clampex) and analysis (Clampfit) software package (Molecular Devices, Sunnyvale, CA, USA) as described in detail in previous papers[17, 32]. The perforated patch technique is a non-invasive electrophysiological recording technique that widely maintains the intracellular milieu of the cell and which is thus in this respect superior to whole cell mode measurements. Electrodes were manufactured from borosilicate capillaries (GB150-8P, Science Products, Hofheim, Germany) using a Sutter P97 horizontal puller (Sutter Instrument Company, Novato, CA, USA). Tip resistances lay between 3.5 and 5 MΩ. The pipette solution contained (in mM) 120 potassium gluconate, 1.5 sodium gluconate, 3.5 NaCl, 1.5 $CaCl_2$, 0.25 $MgCl_2$, 10 HEPES, 10 glucose and 5 EGTA. pH was adjusted to 7.3 by KOH. As the pore forming agent, 500 μg/ml amphotericin B (from Streptomyces sp., compound purchased from Sigma-Aldrich, Vienna, Austria) was added to the pipette solution just prior to each experiment. Experiments were started only after the series resistance had dropped to the lowest achievable level (e.g. to between 20 and 30 MΩ), which usually occurred within 15 to 30 minutes. During the recordings, neurons were continuously superfused using a DAD-12 drug application system (Adams & List, Westbury, NY, USA) with a micromanifold that held 12 channels converging into a 100 μM diameter quartz outlet. The tip of the outlet was positioned in close proximity (about 250 μm) to the patch-clamped cell [Fig. S2]. The standard external solution, which was used as the bathing solution of the cultures during experimentation and as the basal superfusion solution contained (in mM) 140 NaCl, 3 KCl, 2 $CaCl_2$, 2 $MgCl_2$, 10 HEPES, 20 glucose (pH was adjusted to 7.4 by NaOH). Since dihydropyridines (BayK, isradipine) were dissolved in DMSO, the concentration of this solvent was kept constant at 0.3% in the superfusion solutions. Control solution hence contained 0.3% DMSO only, whereas DMSO-soluble compounds were diluted from concentrated stock solutions so as to obtain the same final concentration of DMSO.

PDS induction assays

The $GABA_A$ receptor antagonist bicuculline has been widely used to experimentally evoke PDS (see for example[14, 16, 42, 43]). It mimics the antagonistic effect on the $GABA_A$ receptor of high concentrations of penicillin, which was used in the first reports of PDS *in vivo* [18]. The pleiotropic agent caffeine, which acts on intracellular Ca^{2+} release, on various membrane receptors and as a phosphodiesterase inhibitor[44], was used previously to investigate PDS in hippocampal neurons[45] and was thus included as an alternative means of PDS induction in this study. Both bicuculline (in about two thirds of the neurons, but see the chapter on bicuculline-induced “seizure-like activity” in the Results section) and caffeine are reliable agents for induction of PDS, provided that LTCC are available, or ideally, potentiated ([14, 16, 17, 45] and data shown in Fig. S3A-S3C). These drugs mimic pathogenic processes that have been implicated from research on animal models in the early stages of insult-induced epileptogenesis, i.e. dysfunctional GABAergic inhibition (bicuculline) and - among other effects - disruption of intracellular Ca^{2+} homeostasis (caffeine) (see for example[33, 46]). The sequence of drug application in these PDS-induction assays was as

follows: in the 10 μM bicuculline (BIC)-assay of PDS induction, BIC was applied together with DMSO for 5 minutes, followed by BIC together with BayK for 3 minutes, followed by BIC together with isradipine for another 5 minutes. In the 1 mM caffeine (Caff)-assay of PDS induction, Caff was applied together with DMSO for 5 minutes, followed by Caff together with BayK for 5 minutes, followed by Caff together with isradipine for another 5 minutes. To protect the light-sensitive dihydropyridines from degradation, the reservoirs of the DAD-application system containing the test solutions were kept under impervious cover throughout the experiments. BayK and isradipine were used at low micromolar concentrations (e.g. 3 μM). It has been demonstrated that in this concentration range, $Ca_v1.2DHP^{-/-}$ channels are not potentiated by BayK but can still be inhibited by isradipine[31]. This difference in residual sensitivity may be due to the more complex structural requirements that are required for effective stimulation by dihydropyridine agonists than for the action of antagonists[47]. In line with this notion, no nonspecific activating effect has been found for the dihydropyridine-type LTCC agonist BayK, while dihydropyridine-type LTCC antagonists may act also on other calcium channels (see for example[48]).

Drugs and chemicals

Bay K8644, bicuculline methiodide, caffeine, isradipine, riluzole, CNQX, dimethyl sulfoxide (DMSO), cytosine arabinoside, poly-D-lysine and bulk chemicals were purchased from Sigma-Aldrich (Vienna, Austria). Tetrodotoxin was obtained from Latoxan (Valence, France).

Data analysis and presentation

For identification of spontaneously occurring suprathreshold excitatory events, a threshold search operation („event detection“) was performed using Clampfit 10.2 with the threshold set to 35 mV and re-arm to 5 mV (PDS analysis) or 1 mV (analysis of seizure-like activity) above baseline. This was done for 2 minute periods of each of the above mentioned drug application sequences (i.e. the fourth and fifth minute of DMSO application, the second and third minute of BayK application and the fourth and fifth minute of isradipine application). Prior to event detection, traces were corrected in Clampfit 10.2 for event-of-interest-independent changes of the membrane voltage by manual baseline adjustment (= the dashed grey line in panels A and B of Figs. 2, 3 and 5). Detected events were then analysed for area-below-the-voltage-trajectory, subsequently termed solely “area” (given in mV x ms) and for event duration (given in ms). The analysis of afterdepolarizations depicted in Fig. 4 was performed by evaluation of the area between the curve (starting 7.5 ms after the current injection) and a virtual baseline corresponding to the membrane voltage just prior to stimulation. Preparation of graphs (all data are represented as means ± SEM, unless otherwise stated) and statistical testing (Kruskal-Wallis test with Dunn’s multiple comparison post test, except for data in Fig 4C, where Mann-Whitey test was used) was performed with GraphPad Prism version 5.04. In the statistical analysis, P-values < 0.05 were considered to indicate significant differences between compared data, and P-values ≤ 0.001 were labelled in the graphs with three asterisks (***), P-values between 0.001 and 0.01 with two asterisks (**), and P-values between 0.01 and 0.05 with one asterisk (*). Statistical data comparison yielding P-values ≥ 0.05 was considered to indicate a lack of

statistically significant difference. This applies for all sets of data, where bars are not linked with a horizontal bracket in the graphs.

Results

To address the relative contribution of $Ca_v1.2$ and $Ca_v1.3$ channels to PDS, we compared neurons of $Ca_v1.3^{-/-}$ mice and $Ca_v1.2DHP^{-/-}$ mice with respect to PDS formation using two induction assays (data are summarized in table 1).

Bicuculline-induced PDS

In the first PDS-induction assay, bicuculline was used at a concentration of 10 μM. Recordings were made consecutively during co-administration of solvent (DMSO), 3 μM BayK or 3 μM isradipine. Distinct PDS with spike inactivation and plateau phase emerged after potentiation of LTCCs with BayK in $Ca_v1.2DHP^{-/-}$ neurons (an example is depicted in Fig. 2A), but not in $Ca_v1.3^{-/-}$ neurons (an example is depicted in Fig. 2B). All suprathreshold events recorded under control (DMSO) and the two LTCC-modulating conditions (BayK, isradipine) were analysed with respect to area-below-the-curve (“area”, given in mV x ms) and event length (“duration”, given in ms). Data from $Ca_v1.2DHP^{-/-}$ neurons (n=17) demonstrate pronounced augmentation under BayK by significant larger areas (35% augmentation) and durations (32% augmentation) (Fig. 2C and 2E and table 1) as compared to recordings made in the presence of DMSO. In the presence of isradipine both area and duration were reduced below the DMSO values (area: -20%, duration -10%).

In contrast, although BayK also significantly enhanced suprathreshold events in $Ca_v1.3^{-/-}$ neurons (n=18), the changes were considerably smaller. Both the area and the duration of suprathreshold events were enhanced by 4%, an effect that was only fully restored to the DMSO level with respect to area (± 0%) but not duration in the presence of isradipine (+3%) (Fig. 2D and 2F and table 1). Notably, a distinct plateau phase was only present in the PDS recorded in $Ca_v1.2DHP^{-/-}$ neurons, but not in suprathreshold events of $Ca_v1.3^{-/-}$ neurons, and was due to potentiation of LTCCs as can be seen in exemplary overlays of traces recorded under superfusion of the neurons with DMSO, BayK and isradipine (Fig. 2G and 2H). To obtain information about the size of the most pronounced suprathreshold events evoked in these neurons, we also examined the 95th percentile values, which amounted to 9523 mV x ms in BayK-treated $Ca_v1.2DHP^{-/-}$ neurons, but only 5077 mV x ms in BayK-treated $Ca_v1.3^{-/-}$ neurons.

Caffeine-induced PDS

Experiments as above were repeated using 1 mM caffeine instead of bicuculline as an alternative means of evoking PDS[45]. Again, distinct PDS emerged after potentiation of LTCCs with BayK in $Ca_v1.2DHP^{-/-}$ neurons (an example is depicted in Fig. 3A), but not in $Ca_v1.3^{-/-}$ neurons (an example is depicted in Fig. 3B). Data from $Ca_v1.2DHP^{-/-}$ neurons (n=11) demonstrate pronounced augmentation of suprathreshold events under BayK by significant larger areas (57% augmentation) and durations (38% augmentation) of suprathreshold events (Fig. 3C and 3E and table 1) as compared to recordings made in the presence of DMSO. Exchange of BayK for isradipine diminished the effects seen with

BayK, but failed to restore the control values of DMSO recordings; both area and duration remained enhanced by 22% (area) and 31% (duration). In contrast, although BayK also significantly enhanced suprathreshold events in $Ca_v1.3^{-/-}$ neurons (n=12), the changes were again smaller. The area and the duration of suprathreshold events were enhanced by 42% and 33%. Here, both effects were reversed below the DMSO levels, i.e. -32% (area) and -27% (duration), respectively (Fig. 3D and 3F and table 1). As with bicuculline-induced PDS, a distinct plateau phase was only present in the PDS recorded in $Ca_v1.2DHP^{-/-}$ neurons, but not in $Ca_v1.3^{-/-}$ neurons, and was again due to potentiation of LTCCs as can be seen in exemplary overlays of traces recorded under superfusion of the neurons with DMSO, BayK and isradipine (Fig. 3G and 3H and table 1). The 95th percentile values amounted to 5687 mV x ms in BayK-treated $Ca_v1.2DHP^{-/-}$ neurons, but only 2581 mV x ms in BayK-treated $Ca_v1.3^{-/-}$ neurons.

The data suggest that $Ca_v1.3$ is responsible for mediating the LTCC-dependent part of PDS. It is a widespread belief that Ca^{2+}-dependent cation (CAN) channels also play a crucial role in PDS formation, and this view is well documented in textbooks on the basic mechanisms of epilepsy (see Fig. 1). However, a contribution of CAN conductance to PDS has never been proven experimentally. This is largely due to the lack of knowledge regarding the molecular nature of CAN channels (which have been identified solely on a mechanistic basis) and consequently the absence of specific channel inhibitors. Notably, we demonstrated in a previous study that $Ca_v1.2$ channels (but not $Ca_v1.3$ channels) couple functionally to CAN channels, which gives rise to afterdepolarizations (ADPs)[29]. A new summarizing analysis of this finding is illustrated in Fig. 4. In the presence of BayK the repolarizing voltage trajectories after the current injection covered an average area of 14419 ± 7577 mV x ms in $Ca_v1.3^{-/-}$ neurons (n=10), but of only 1029 ± 201 mV x ms in $Ca_v1.2DHP^{-/-}$ neurons (n=15) (see the inserts in Fig. 4D and 4E). These areas are significantly larger (P-values ≤ 0.001) than in the presence of isradipine in $Ca_v1.3^{-/-}$ neurons (313 ± 51 mV x ms), but not in $Ca_v1.2DHP^{-/-}$ neurons (551± 91 mV x ms, P value > 0.05), which demonstrates the presence of distinct LTCC-dependent ADPs in $Ca_v1.3^{-/-}$ neurons, but not in $Ca_v1.2DHP^{-/-}$ neurons. In earlier work we showed that these ADPs were due to Na^+-influx via calcium-dependent, flufenamic-acid-sensitive channels (i.e. CAN channels)[32]. These experiments were performed in the presence of tetrodotoxin (TTX) to allow for a better control of the depolarization range induced by the current injections. Thus, action potential firing was disabled. However, it should be noted that PDS only show overshooting action potential discharge at their onset. As described already in the earliest reports, this phase is followed a “progressive decrease in amplitude until only small oscillations remained riding on top of the PDS”[18]. Hence, slow voltage-trajectories dominate most of the depolarizing shift. Therefore, the results obtained in TTX-silenced neurons regarding LTCC-CAN-coupling may largely apply also to the situation in PDS. However, since we could not rule out that non-L-type HVA-mediated Ca^{2+}- influx during spike discharge might enable an (LTCC-independent) activation of CAN channels during the depolarizing shift, we repeated the experiments illustrated in Fig. 4 in the absence of TTX. For clarity, 10 μM of the AMPA-receptor inhibitor CNQX were added to avoid network-derived distortion of neuronal firing patterns. As illustrated in Fig. S4 and Fig. S5, distinct ADPs were again elicited in $Ca_v1.3^{-/-}$

neurons only, but not in $Ca_v1.2DHP^{-/-}$ neurons. The lack of ADPs in isradipine-treated $Ca_v1.3^{-/-}$ neurons demonstrates an absence of non-LTCC-CAN channel coupling.

Hence, if CAN channels do indeed play a role in PDS, these events should be prominent in neurons which do show LTCC-CAN coupling, i.e. neurons derived from $Ca_v1.3^{-/-}$ mice, where $Ca_v1.2$-CAN coupling gives rise to pronounced ADPs, in particular when $Ca_v1.2$ is potentiated by BayK[29]. On the other hand, PDS should be considerably smaller in neurons that express only dihydropyridine-insensitive $Ca_v1.2$ channels derived from $Ca_v1.2DHP^{-/-}$ mice, in which BayK thus failed to evoke distinct ADPs. The fact that the opposite was the case, i.e. pronounced PDS upon application of BayK in $Ca_v1.2DHP^{-/-}$ neurons, but no distinct PDS in Cav1.3-/- neurons, suggests that PDS do not require an activation of CAN channels to occur.

Physiologically, CAN channels were reported to underlie prolonged neuronal discharge patterns[49, 50, 51, 52]. As for epileptiform discharges, we wondered - if not in PDS - in which other discharge pattern the $Ca_v1.2$-CAN channel coupling may come into play.

Bicuculline-induced seizure-like activity

Experiments also using bicuculline allowed us to address this question. As described previously in hippocampal slices, bicuculline typically induced an initial prolonged depolarization (the “primary burst”) which successively turned into PDS discharge[53]. However, in a subpopulation of neurons (~ 1/3), no such transition occurred, but the neurons continued to generate burst-like discharges, which we tentatively designated as “seizure-like activity” (SLA) to emphasize its difference to PDS (Fig. 5, top traces). Hence we could test for a role of LTCC-CAN coupling on long-lasting neuronal activities (i.e. ≥ 3 s). When evoked in the presence of BayK, bicuculline-induced SLA appeared similar on gross examination in $Ca_v1.2DHP^{-/-}$ and in $Ca_v1.3$-/- neurons (Fig. 5A and 5B). However, modulating LTCC activity using dihydropyridines revealed essential differences. SLA in $Ca_v1.2DHP^{-/-}$neurons (n=10) appeared largely independent of LTCCs, because both the event area (BayK: -4%; isradipine: -15%) as well as the event duration (BayK: +7%; isradipine: -2%) were only slightly affected by administration of BayK and isradipine (Fig. 5C and 5E and table 1). In contrast, SLA in $Ca_v1.3^{-/-}$ neurons (n=10) showed an obvious LTCC-dependent component, in that both event area (BayK: +48%; isradipine: -31%) and event duration (BayK: +36%; isradipine: -26%) were augmented by BayK and reduced by isradipine (Fig. 5D and 5F and table 1). The effect or lack of effect of LTCC modulation is illustrated in Fig. 5G and 5H by overlays of SLA traces recorded under control condition (DMSO), in the presence of BayK and after exchange of BayK for isradipine. Hence, here the situation was just the opposite as for the brief (up to several hundred ms-long) PDS. SLA was evidently augmented by BayK in $Ca_v1.3^{-/-}$ neurons (Fig. 5B, 5D), but not in $Ca_v1.2DHP^{-/-}$ neurons (Fig. 5A, 5C).

Europe PMC Funders Author Manuscripts

Discussion

$Ca_V1.3$ channels mediate the L-type voltage-gated calcium channel-dependent component of paroxysmal depolarization shifts

In this study we investigated the molecular nature of LTCCs contributing to PDS. Additionally, previous findings[29] allowed us to test the alleged role of CAN channels[28].

The induction of prominent PDS in $Ca_V1.2DHP^{-/-}$ neurons by BayK indicates the involvement of $Ca_V1.3$ channels. Indeed, in neurons devoid of $Ca_V1.3$ channels, distinct PDS were not elicited. What could determine the preferential role of $Ca_V1.3$ rather than $Ca_V1.2$ in PDS? Broadly speaking, $Ca_V1.2$ and $Ca_V1.3$ channels have similar neuronal distribution and physiological functions. However, there appear to be essential differences on close examination. While both neuronal LTCCs are localized in the somatodendritic compartment, they differ with respect to cluster formation and association with synaptic sites (reviewed in[39]). And while both neuronal LTCCs play a role in the regulation of neuronal excitability, there are differences with respect to the coupling of LTCC-mediated Ca^{2+}-influx to Ca^{2+}-dependent conductances[29]. However, the most stressed difference between $Ca_V1.2$ and $Ca_V1.3$ relates to their voltage-dependent activation. $Ca_V1.3$ channels have been shown to open at more hyperpolarized voltages than those typically required to open $Ca_V1.2$ channels (reviewed in[7]), although we have recently obtained evidence that some $Ca_V1.2$ channels may also operate in a similar hyperpolarized voltage range[29]. However, since voltage-dependent inactivation appears less different between $Ca_V1.2$ and $Ca_V1.3$ channels, $Ca_V1.3$ channels can be envisaged to carry significant window current during prolonged depolarization[54]. The capability to carry significant window current may enable $Ca_V1.3$ channels to mediate the plateau phase of PDS, without the necessity to involve CAN channels. Since only $Ca_V1.2$ channels, but not $Ca_V1.3$ channels couple to CAN channels, our data indeed strongly argue against a role of CAN channels in PDS formation, and thus seriously question current textbook schemes on PDS formation.

Potential limitations

For reasons outlined in the Methods section an in vitro model was used in this study. A disadvantage of this model system is that the precise maturation state as well as the consistency of inherent hippocampal characteristics of the cultured neurons remain largely undefined. However, PDS do not appear to be restricted to a certain class of brain neurons[13, 16, 41, 43] nor is there any evidence that their occurrence is limited to a certain age.

It should be noted that we performed our experiments on continuously superfused hippocampal neurons. Neuronal activity in this preparation is largely controlled by endogenous conductances and fast excitatory and inhibitory synaptic inputs, but largely lacks neuromodulatory influences. Hence, our experiments addressed the primary mechanisms of PDS formation. Our data do not rule out the possibility that neuromodulatory alterations enable additional conductances (e.g. metabotropically activated CAN channels) to further prolong PDS or to eventually even cause transition to seizure-like discharge activity. Indeed, metabotropic glutamate receptor (mGluR)-mediated activation of canonical transient receptor potential channels (TRPC channels[55]) generated large depolarizing plateau

potentials that were similar in overall shape to PDS, although they considerably exceeded in duration those originally recorded in pre-seizure penicillin-induced foci[18]. Notably, a similar mGluR-activated CAN conductance was suggested to play a role in neuronal network synchronization[56].

A role for $Ca_v1.3$ in the early stages of epileptogenesis?

However, early PDS appear to rely largely on Ca^{2+}-influx via $Ca_v1.3$ channels. Because PDS have been implicated in the processes leading to epilepsy[25, 27] our study now provides a possible mechanistic link between $Ca_v1.3$ enhancement and epileptogenesis. Intriguingly, although both neuronal LTCCs ($Ca_v1.2$ and $Ca_v1.3$) play a role in excitation-transcription coupling, they seem to differ somewhat in their capability to induce phosphorylation of cAMP responsive element-binding protein (CREB) phosphorylation, with $Ca_v1.3$ being more effective than $Ca_v1.2$[57]. Hence, pulsative Ca^{2+} rises provided by $Ca_v1.3$ channels may potentially trigger epileptogenic remodelling processes. This possibility needs to be further addressed in the future.

In line with a role in epileptogenesis, an early up-regulation of $Ca_v1.3$ was observed in the pilocarpine-induced status epilepticus model of acquired epilepsy[58]. Also in status epilepticus models of acquired epilepsy, electrographic spikes (the multi-unit correlate of PDS) were found to appear immediately after the injury[26, 59, 60]. These spikes were described as stereotyped at an early stage of epileptogenesis, but their shape gradually changed within the weeks that follow the initial lesion[26, 60]. Since a decrease of GABAergic inhibition has been identified as an early mechanism of electrographic spike generation (see for example[46]), we suggest that bicuculline may induce a relatively simple, primordial type of PDS. In line with a role of LTCCs in primordial PDS, the brain permeant dihydropyridine-type LTCC antagonist nimodipine, when given only in the acute stage of an animal model of acquired epilepsy, showed a protective effect against subsequent spontaneous recurrent seizures, which indicates an (early) anti-epileptogenic effect[61]. It remains to be seen whether PDS at this stage have the capability to modify other conductances, such as the one underlying $I_{Na,p}$. $I_{Na,p}$ was suggested to be mostly of perisomatic origin (see[62] and citations therein). There is strong evidence that $I_{Na,p}$ plays a role in epilepsy (reviewed in[63]), but it may be recruited at later stages of epileptogenesis[64]. Notably, inhibition of $I_{Na,p}$, by low concentrations of riluzole did not affect PDS investigated in this study, but inhibited seizure-like activity (see Fig. S6).

Because of the uncertainty about the molecular nature of CAN channels, it remains unclear whether a similar situation may also apply for I_{CAN}. However, bicuculline-induced long-lasting epileptiform discharges (“SLA”) were prolonged by BayK in $Ca_v1.3^{-/-}$ neurons, but not in $Ca_v1.2DHP^{-/-}$ neurons. This effect can be envisaged to represent a pathophysiological correlate of the proposed physiological role of CAN channels in generation of burst discharges and plateau potentials[49, 51]. Moreover, with somatic current injections a depolarized plateau was more easily elicited by BayK in $Ca_v1.3^{-/-}$ neurons than in $Ca_v1.2DHP^{-/-}$ neurons (see Fig. S4A, B and Fig. S5A, B), which suggests prominent $Ca_v1.2$-CAN channel coupling at the cell soma. In neocortical neurons, I_{CAN} was shown to enable runs of PDS by generating a slow depolarizing waveform. When CAN channels were

blocked, individual (unaltered) PDS remained[43]. Hence, $I_{Na,p}$ and I_{CAN} may play a role in the generation of more complex patterns of epileptiform activity, i.e. seizure-like activity, but do not crucially contribute to PDS.

Conclusion and Outlook

Our data indicate that primordial PDS (those occurring immediately after injury, way before the occurrence of unprovoked seizures) may in principle be less complex in mechanistic terms than previously thought. Here we demonstrated that potentiation of $Ca_v1.3$ sufficed for their induction when ionotropic GABAergic inhibition was compromised. Similar results with caffeine indicate that the implication of $Ca_v1.3$ in PDS may apply to various PDS-precipitating mechanisms. The crucial role of $Ca_v1.3$ channels provides an interesting target for PDS prevention, which may be a strategy to attenuate or impede epileptogenesis at an early stage. Obviously, the proposed epileptogenic role of $Ca_v1.3$ needs to be further tested in the future in appropriate animal models of epileptogenesis. Our results provide the necessary *in vitro* data to justify and refine the required *in vivo* animal research.

To date, no isoform selective LTCC inhibitors are available to date for target-directed therapeutic approaches. However, accumulating evidence of a crucial role of $Ca_v1.3$ channels in Parkinson's disease has already triggered efforts to identify specific inhibitors[65]. It remains to be seen whether the compounds proposed so far do indeed prove to be isoform-selective in various independent studies, and in particular on native LTCCs. Unfortunately, serious doubts have been raised regarding these compounds recently[66]. Our findings may further encourage the search for truly $Ca_v1.3$ selective antagonists.

Supplementary Material

Refer to Web version on PubMed Central for supplementary material.

Acknowledgements

We would like to acknowledge support of this study by a grant of the Herzfelder'sche Familienstiftung as well as by the Austrian Science Fund (FWF, project P28179), both to H.K. Furthermore, we thank Gabriele Gaupmann for excellent technical assistance and Assoc. Prof. Dr. Marion Bankstahl (Department of Pharmacology, Toxicology, and Pharmacy, University of Veterinary Medicine Hannover, Germany) for advice in the early stage of writing the manuscript and for valuable suggestions.

References

1. Calin-Jageman I, Lee A. Ca_v1 L-type Ca^{2+} channel signaling complexes in neurons. J Neurochem. 2008; 105:573–583. [PubMed: 18266933]
2. Zhang Z, Séguéla P. Metabotropic induction of persistent activity in layers II/III of anterior cingulate cortex. Cereb Cortex. 2010; 20:2948–2957. [PubMed: 20348157]
3. Pérez-Garci E, Larkum ME, Nevian T. Inhibition of dendritic Ca^{2+} spikes by GABAB receptors in cortical pyramidal neurons is mediated by a direct Gi/o-β-subunit interaction with Cav1 channels. J Physiol. 2013; 591:1599–1612. [PubMed: 23184512]
4. Kulak W, Sobaniec W, Wojtal K, et al. Calcium modulation in epilepsy. Pol J Pharmacol. 2004; 56:29–41. [PubMed: 15047975]
5. Amano H, Amano T, Matsubayashi H, et al. Enhanced calcium influx in hippocampal CA3 neurons of spontaneously epileptic rats. Epilepsia. 2001; 42:345–350. [PubMed: 11442151]

6. Yan HD, Ishihara K, Hanaya R, et al. Voltage-dependent calcium channel abnormalities in hippocampal CA3 neurons of spontaneously epileptic rats. Epilepsia. 2007; 48:758–764. [PubMed: 17326796]
7. Lipscombe D, Helton TD, Xu W. L-type calcium channels: the low down. J Neurophysiol. 2004; 92:2633–2641. [PubMed: 15486420]
8. Park SK, Hwang IK, An SJ, et al. Elevated P/Q type (alpha1A) and L2 type (alpha1D) Purkinje cell voltage-gated calcium channels in the cerebella of seizure prone gerbils. Mol Cells. 2003; 16:297–301. [PubMed: 14744018]
9. N'Gouemo P, Yasuda R, Faingold CL. Seizure susceptibility is associated with altered protein expression of voltage-gated calcium channel subunits in inferior colliculus neurons of the genetically epilepsy-prone rat. Brain Res. 2010; 1308:153–157. [PubMed: 19836362]
10. Kanyshkova T, Ehling P, Cerina M, et al. Regionally specific expression of high-voltage-activated calcium channels in thalamic nuclei of epileptic and non-epileptic rats. Mol Cell Neurosci. 2014; 61:110–122. [PubMed: 24914823]
11. Klassen T, Davis C, Goldman A, et al. Exome sequencing of ion channel genes reveals complex profiles confounding personal risk assessment in epilepsy. Cell. 2011; 145:1036–1048. [PubMed: 21703448]
12. Pinggera A, Striessnig J. Ca_v 1.3 (CACNA1D) L-type Ca^{2+} channel dysfunction in CNS disorders. J Physiol. 2016; 594:5839–5849. [PubMed: 26842699]
13. Walden J, Pockberger H, Speckmann EJ, et al. Paroxysmal neuronal depolarizations in the rat motorcortex in vivo: intracellular injection of the calcium agonist BAY K 8644. Exp Brain Res. 1986; 64:607–609. [PubMed: 2433141]
14. Straub H, Speckmann EJ, Bingmann D, et al. Paroxysmal depolarization shifts induced by bicuculline in CA3 neurons of hippocampal slices: suppression by the organic calcium antagonist verapamil. Neurosci Lett. 1990 Mar 26; 111(1-2):99–101. [PubMed: 2336199]
15. Momiyama T, Ishihara K, Serikawa T, et al. Effect of nicardipine on abnormal excitability of CA3 pyramidal cells in hippocampal slices of spontaneously epileptic rats. Eur J Pharmacol. 1995 Jul 4; 280(2):119–23. [PubMed: 7589175]
16. Schiller Y. Inter-ictal- and ictal-like epileptic discharges in the dendritic tree of neocortical pyramidal neurons. J Neurophysiol. 2002; 88:2954–2962. [PubMed: 12466421]
17. Rubi L, Schandl U, Lagler M, et al. Raised activity of L-type calcium channels renders neurons prone to form paroxysmal depolarization shifts. Neuromolecular Med. 2013; 15:476–492. [PubMed: 23695859]
18. Matsumoto H, Ajmone Marsan C. Cortical cellular phenomena in experimental epilepsy: interictal manifestations. Exp Neurol. 1964; 9:286–304. [PubMed: 14145629]
19. Jefferys JG. Basic mechanisms of focal epilepsies. Exp Physiol. 1990; 75:127–162. [PubMed: 2111151]
20. Holmes GL, Ben-Ari Y. The neurobiology and consequences of epilepsy in the developing brain. Pediatr Res. 2001; 49:320–325. [PubMed: 11228256]
21. Ben-Ari Y, Cherubini E, Corradetti R, et al. Giant synaptic potentials in immature rat CA3 hippocampal neurones. J Physiol. 1989; 416:303–325. [PubMed: 2575165]
22. Prince DA. The depolarization shift in "epileptic" neurons. Exp Neurol. 1968; 21:467–485. [PubMed: 5677264]
23. Mantegazza M, Franceschetti S, Avanzini G. Anemone toxin (ATX II)-induced increase in persistent sodium current: effects on the firing properties of rat neocortical pyramidal neurones. J Physiol. 1998; 507:105–116. [PubMed: 9490824]
24. Chen S, Su H, Yue C, et al. An increase in persistent sodium current contributes to intrinsic neuronal bursting after status epilepticus. J Neurophysiol. 2011; 105:117–129. [PubMed: 20980543]
25. Staley K, Hellier JL, Dudek FE. Do interictal spikes drive epileptogenesis? Neuroscientist. 2005; 11:272–276. [PubMed: 16061513]
26. Chauvière L, Doublet T, Ghestem A, et al. Changes in interictal spike features precede the onset of temporal lobe epilepsy. Ann Neurol. 2012; 71:805–814. [PubMed: 22718546]

27. Staley KJ, White A, Dudek FE. Interictal spikes: harbingers or causes of epilepsy? Neurosci Lett. 2011; 497:247–250. [PubMed: 21458535]
28. Speckmann, EJ, Walden, J. Anti-epileptic effects of organic calcium channel blockersEpilepsy: Models, Mechanisms and Concepts. Schwartzkroin, PA, editor. Vol. 1993. University Press; Cambridge: 1993. 462–486.
29. Hasreiter J, Goldnagl L, Böhm S, et al. $Ca_V1.2$ and $Ca_V1.3$ L-type calcium channels operate in a similar voltage range but show different coupling to Ca^{2+}-dependent conductances in hippocampal neurons. Am J Physiol Cell Physiol. 2014; 306:C1200–C1213. [PubMed: 24760982]
30. Platzer J, Engel J, Schrott-Fischer A, et al. Congenital deafness and sinoatrial node dysfunction in mice lacking class D L-type Ca^{2+} channels. Cell. 2000; 102:89–97. [PubMed: 10929716]
31. Sinnegger-Brauns MJ, Hetzenauer A, Huber IG, et al. Isoform-specific regulation of mood behavior and pancreatic beta cell and cardiovascular function by L-type Ca^{2+} channels. J Clin Invest. 2004; 113:1430–1439. [PubMed: 15146240]
32. Geier P, Lagler M, Boehm S, et al. Dynamic interplay of excitatory and inhibitory coupling modes of neuronal L-type calcium channels. Am J Physiol Cell Physiol. 2011; 300:C937–C949. [PubMed: 21228322]
33. DeLorenzo RJ, Sun DA, Deshpande LS. Erratum to “Cellular mechanisms underlying acquired epilepsy: the calcium hypothesis of the induction and maintenance of epilepsy.”. Pharmacol Ther. 2006; 111:288–325. [PubMed: 16832874]
34. Kovács R, Kardos J, Heinemann U, et al. Mitochondrial calcium ion and membrane potential transients follow the pattern of epileptiform discharges in hippocampal slice cultures. J Neurosci. 2005; 25:4260–4269. [PubMed: 15858052]
35. Segal MM, Furshpan EJ. Epileptiform activity in microcultures containing small numbers of hippocampal neurons. J Neurophysiol. 1990; 64:1390–1399. [PubMed: 2283535]
36. Segal MM. Epileptiform activity in microcultures containing one excitatory hippocampal neuron. J Neurophysiol. 1991; 65:761–770. [PubMed: 1646871]
37. Staley KJ, Dudek FE. Interictal spikes and epileptogenesis. Epilepsy Curr. 2006; 6:199–202. [PubMed: 17260059]
38. Rogawski MA. Point-counterpoint: Do interictal spikes trigger seizures or protect against them? Epilepsy Curr. 2006; 6:197–198. [PubMed: 17260058]
39. Vacher H, Mohapatra DP, Trimmer JS. Localization and targeting of voltagedependent ion channels in mammalian central neurons. Physiol Rev. 2008; 88:1407–1447. [PubMed: 18923186]
40. Johnston D, Brown TH. The synaptic nature of the paroxysmal depolarizing shift in hippocampal neurons. Ann Neurol. 1984; 16(Suppl):S65–71. [PubMed: 6095744]
41. Witte OW, Speckmann EJ, Walden J. Motor cortical epileptic foci in vivo: actions of a calcium channel blocker on paroxysmal neuronal depolarizations. Electroencephalogr Clin Neurophysiol. 1987; 66:43–55. [PubMed: 2431865]
42. de Curtis M, Radici C, Forti M. Cellular mechanisms underlying spontaneous interictal spikes in an acute model of focal cortical epileptogenesis. Neuroscience. 1999; 88:107–117. [PubMed: 10051193]
43. Schiller Y. Activation of a calcium-activated cation current during epileptiform discharges and its possible role in sustaining seizure-like events in neocortical slices. J Neurophysiol. 2004; 92:862–872. [PubMed: 15277598]
44. Ribeiro JA, Sebastião AM. Caffeine and adenosine. J Alzheimers Dis. 2010; 20(Suppl 1):S3–15. [PubMed: 20164566]
45. Moraidis I, Bingmann D, Lehmenkühler A, et al. Caffeine-induced epileptic discharges in CA3 neurons of hippocampal slices of the guinea pig. Neurosci Lett. 1991; 129:51–54. [PubMed: 1922970]
46. Bouilleret V, Loup F, Kiener T, et al. Early loss of interneurons and delayed subunitspecific changes in GABA(A)-receptor expression in a mouse model of mesial temporal lobe epilepsy. Hippocampus. 2000; 10:305–324. [PubMed: 10902900]
47. Wappl E, Mitterdorfer J, Glossmann H, et al. Mechanism of dihydropyridine interaction with critical binding residues of L-type Ca^{2+} channel alpha 1 subunits. J Biol Chem. 2001; 276:12730–12735. [PubMed: 11278630]

48. Perez-Reyes E, Van Deusen AL, Vitko I. Molecular pharmacology of human $Ca_v3.2$ T-type Ca^{2+} channels: block by antihypertensives, antiarrhythmics, and their analogs. J Pharmacol Exp Ther. 2009; 328:621–627. [PubMed: 18974361]
49. Kramer RH, Zucker RS. Calcium-induced inactivation of calcium current causes the inter-burst hyperpolarization of Aplysia bursting neurones. J Physiol. 1985; 362:131–160. [PubMed: 2410598]
50. Launay P, Fleig A, Perraud AL, et al. TRPM4 is a Ca^{2+}-activated nonselective cation channel mediating cell membrane depolarization. Cell. 2002; 109:397–407. [PubMed: 12015988]
51. Lee CR, Tepper JM. A calcium-activated nonselective cation conductance underlies the plateau potential in rat substantia nigra GABAergic neurons. J Neurosci. 2007; 27:6531–6541. [PubMed: 17567814]
52. Teruyama R, Armstrong WE. Calcium-dependent fast depolarizing afterpotentials in vasopressin neurons in the rat supraoptic nucleus. J Neurophysiol. 2007; 98:2612–2621. [PubMed: 17715195]
53. Borck C, Jefferys JG. Seizure-like events in disinhibited ventral slices of adult rat hippocampus. J Neurophysiol. 1999; 82:2130–2142. [PubMed: 10561393]
54. Xu W, Lipscombe D. Neuronal $Ca_v1.3alpha_1$ L-type channels activate at relatively hyperpolarized membrane potentials and are incompletely inhibited by dihydropyridines. J Neurosci. 2001; 21:5944–5951. [PubMed: 11487617]
55. Zheng F, Phelan KD. The role of canonical transient receptor potential channels in seizure and excitotoxicity. Cells. 2014; 3:288–303. [PubMed: 24722470]
56. Congar P, Leinekugel X, Ben-Ari Y, et al. A long-lasting calcium-activated nonselective cationic current is generated by synaptic stimulation or exogenous activation of group I metabotropic glutamate receptors in CA1 pyramidal neurons. J Neurosci. 1997; 17:5366–5379. [PubMed: 9204921]
57. Zhang H, Fu Y, Altier C, Platzer J, et al. $Ca_v1.2$ and $Ca_v1.3$ neuronal L-type calcium channels: differential targeting and signaling to pCREB. Eur J Neurosci. 2006; 23:2297–2310. [PubMed: 16706838]
58. Xu JH, Long L, Tang YC, et al. $Ca_v1.2$, $Ca_v1.3$, and $Ca_v2.1$ in the mouse hippocampus during and after pilocarpine-induced status epilepticus. Hippocampus. 2007; 17:235–251. [PubMed: 17265461]
59. Hellier JL, Patrylo PR, Dou P, et al. Assessment of inhibition and epileptiform activity in the septal dentate gyrus of freely behaving rats during the first week after kainate treatment. J Neurosci. 1999; 19:10053–10064. [PubMed: 10559413]
60. Huneau C, Benquet P, Dieuset G, et al. Shape features of epileptic spikes are a marker of epileptogenesis in mice. Epilepsia. 2013; 54:2219–2227. [PubMed: 24134559]
61. Mikati MA, Holmes GL, Werner S, et al. Effects of nimodipine on the behavioral sequalae of experimental status epilepticus in prepubescent rats. Epilepsy Behav. 2004; 5:168–174. [PubMed: 15123017]
62. Vervaeke K, Hu H, Graham LJ, et al. Contrasting effects of the persistent Na^+ current on neuronal excitability and spike timing. Neuron. 2006; 49:257–270. [PubMed: 16423699]
63. Stafstrom CE. Persistent sodium current and its role in epilepsy. Epilepsy Curr. 2007; 7:15–22. [PubMed: 17304346]
64. Agrawal N, Alonso A, Ragsdale DS. Increased persistent sodium currents in rat entorhinal cortex layer V neurons in a post-status epilepticus model of temporal lobe epilepsy. Epilepsia. 2003; 44:1601–1604. [PubMed: 14636336]
65. Kang S, Cooper G, Dunne SF, et al. $Ca_v1.3$-selective L-type calcium channel antagonists as potential new therapeutics for Parkinson's disease. Nat Commun. 2012; 3
66. Ortner NJ, Bock G, Vandael DH, et al. Pyrimidine-2,4,6-triones are a new class of voltage-gated L-type Ca^{2+} channel activators. Nat Commun. 2014; 5

Europe PMC Funders Author Manuscripts

Key Points

- $Ca_v1.3$ channels are largely responsible for the L-type voltage-gated calcium channel-mediated component of an original type of paroxysmal depolarization shifts (PDS) in cultured hippocampal neurons.
- Ca^{2+}-dependent nonspecific cation (CAN) channels are not required for formation of this type of PDS.
- CAN channels contribute to long-lasting epileptiform activity
- $Ca_v1.3$ channels may provide a target for PDS elimination

Europe PMC Funders Author Manuscripts

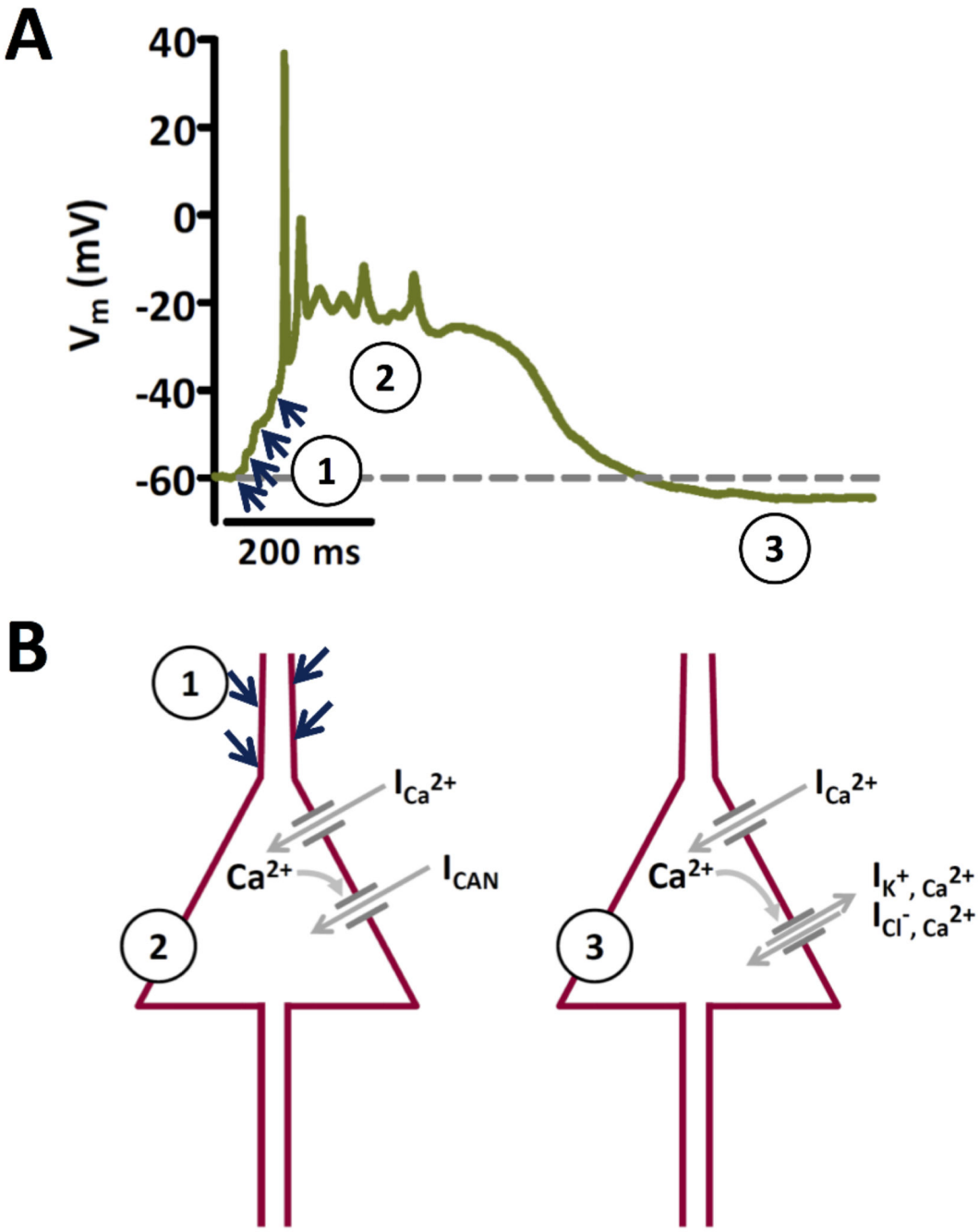

Figure 1. Proposed mechanisms of PDS generation.

A Recording of an original type of PDS that illustrates activation by summing up of excitatory inputs (indicated by the blue arrows) to a giant post-synaptic potential that triggers action potential firing (1), which turns after spike-decline into a plateau phase (2). After the plateau, the membrane potential may return back to baseline (dashed line) or transiently to an even more hyperpolarized potential (afterhyperpolarization) as in the example shown (3). **B** The two schemes illustrate the conductances that have been proposed to underlie the formation of original PDS. Phase 1 in A is mediated by excitatory synaptic

Europe PMC Funders Author Manuscripts

input, presumably via AMPA type glutamate receptors. The decline in action potential amplitude is thought to be due to progressive inactivation of voltage-gated sodium channels. The plateau phase (2) may be largely due to L-type mediated Ca^{2+} inward current ($I_{Ca}{}^{2+}$), allegedly together with cationic inward current via CAN channels (I_{CAN}). Afterhyperpolarizations (3) are considered to be due to K^+-efflux and/or Cl^--influx via Ca^{2+}-activated K^+ and Cl^- channels. Note that this figure is based on a textbook figure published by Speckmann and Walden (1993)[28] to illustrate the proposed role of CAN channels. It has been modified with respect to the prevailing view of an initiation of the PDS by excitatory postsynaptic potentials[20, 38, 40], whereas in the original depiction by Speckmann and colleagues the onset was described to be caused directly by inward calcium current.

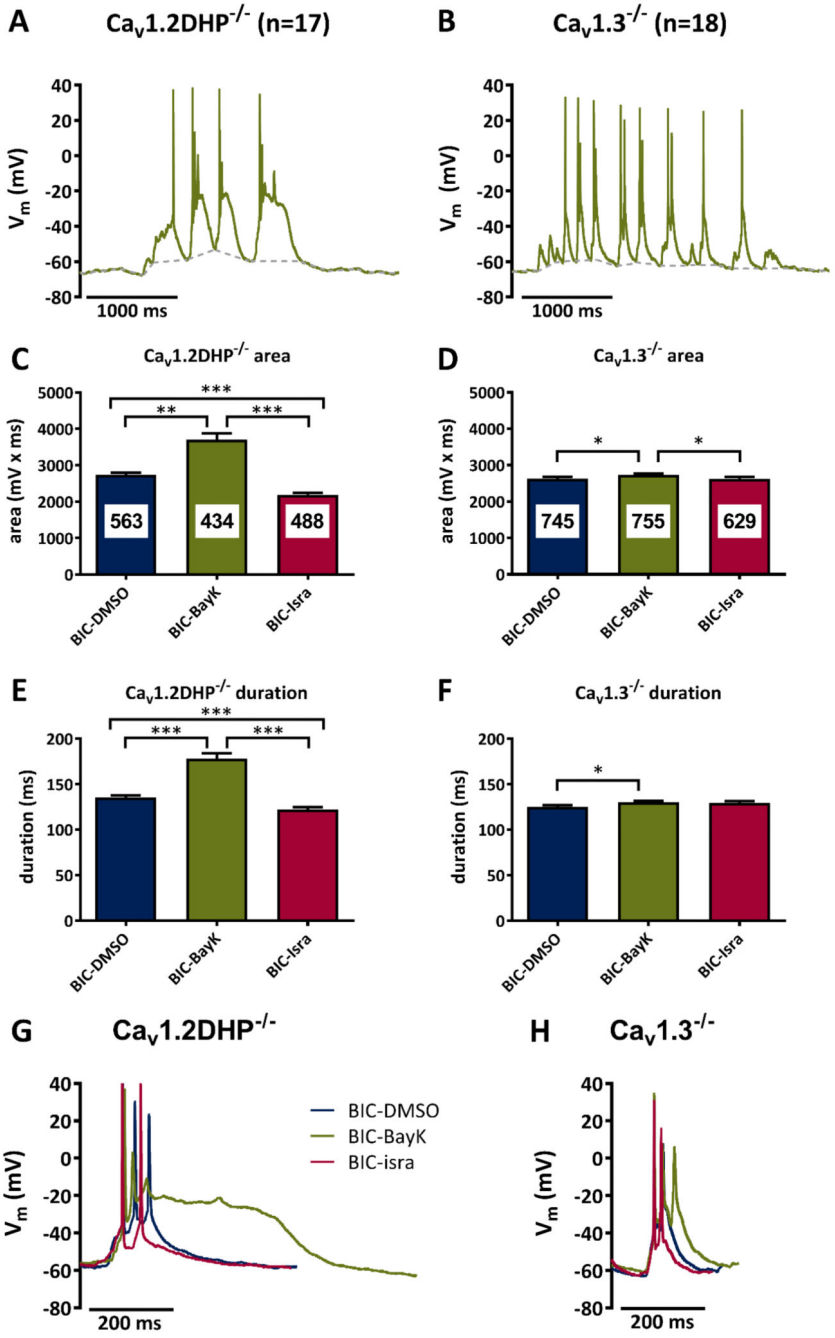

Figure 2. Bicuculline-induced PDS require Ca$_V$1.3 channels.

A, **B** Suprathreshold electrical events recorded in Ca$_V$1.2DHP$^{-/-}$ neurons (A) or Ca$_V$1.3$^{-/-}$ neurons (B) after co-administration of bicuculline (10 μM) and BayK (3 μM). **C-F** Analysis of the area (C, D) and duration (E, F) of all suprathreshold electrical events recorded in the presence of bicuculline in Ca$_V$1.2DHP$^{-/-}$ neurons (C, E) or Ca$_V$1.3$^{-/-}$ neurons (D, F) under three conditions of LTCC activity: endogenous activity (DMSO control), potentiated (BayK, 3 μM) and inhibited (isradipine, 3 μM). The figures in the bars indicate the total number of events evaluated. All statistically significant differences are indicated by horizontal brackets.

G, **H** Overlay of typical suprathreshold electric events recorded from $Ca_v1.2DHP^{-/-}$ neurons (G) or $Ca_v1.3^{-/-}$ neurons (H) from the experiments analysed in C to F.

Europe PMC Funders Author Manuscripts

Europe PMC Funders Author Manuscripts

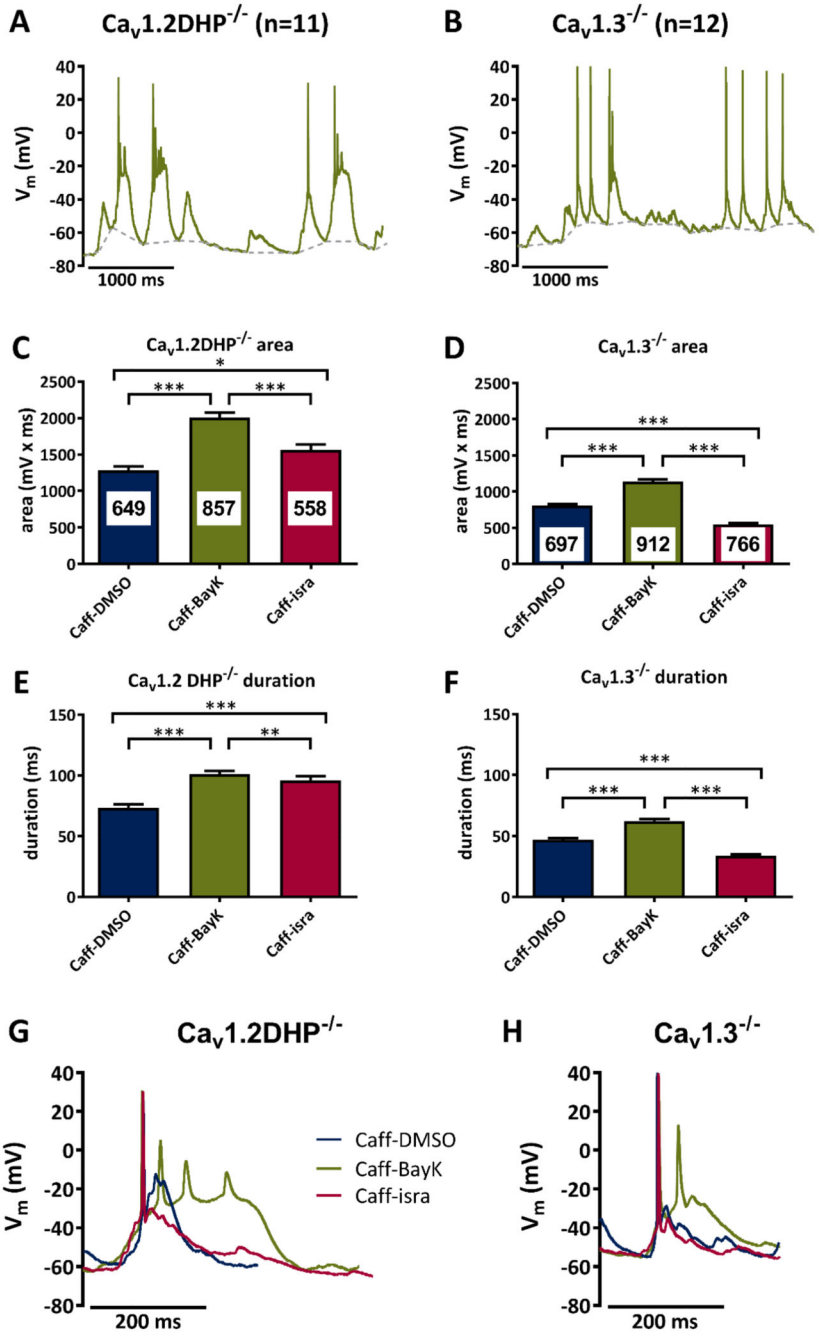

Figure 3. Caffeine-induced PDS require Ca$_v$1.3 channels.

A, **B** Suprathreshold electrical events recorded in Ca$_v$1.2DHP$^{-/-}$ neurons (A) or Ca$_v$1.3$^{-/-}$ neurons (B) after co-administration of caffeine (1 mM) and BayK (3 μM). **C**-**F** Analysis of the area (C, D) and duration (E, F) of suprathreshold electrical events recorded in the presence of caffeine in Ca$_v$1.2DHP$^{-/-}$ neurons (C, E) or Ca$_v$1.3$^{-/-}$ neurons (D, F) under three conditions of LTCC activity: endogenous activity (DMSO control), potentiated (BayK, 3 μM) and inhibited (isradipine, 3 μM). The figures in the bars indicate the total number of events evaluated. All statistically significant differences are indicated by horizontal brackets.

G, **H** Overlay of typical suprathreshold electric events recorded from $Ca_v1.2DHP^{-/-}$ neurons (G) or $Ca_v1.3^{-/-}$ neurons (H) from the experiments analysed in C to F.

Europe PMC Funders Author Manuscripts

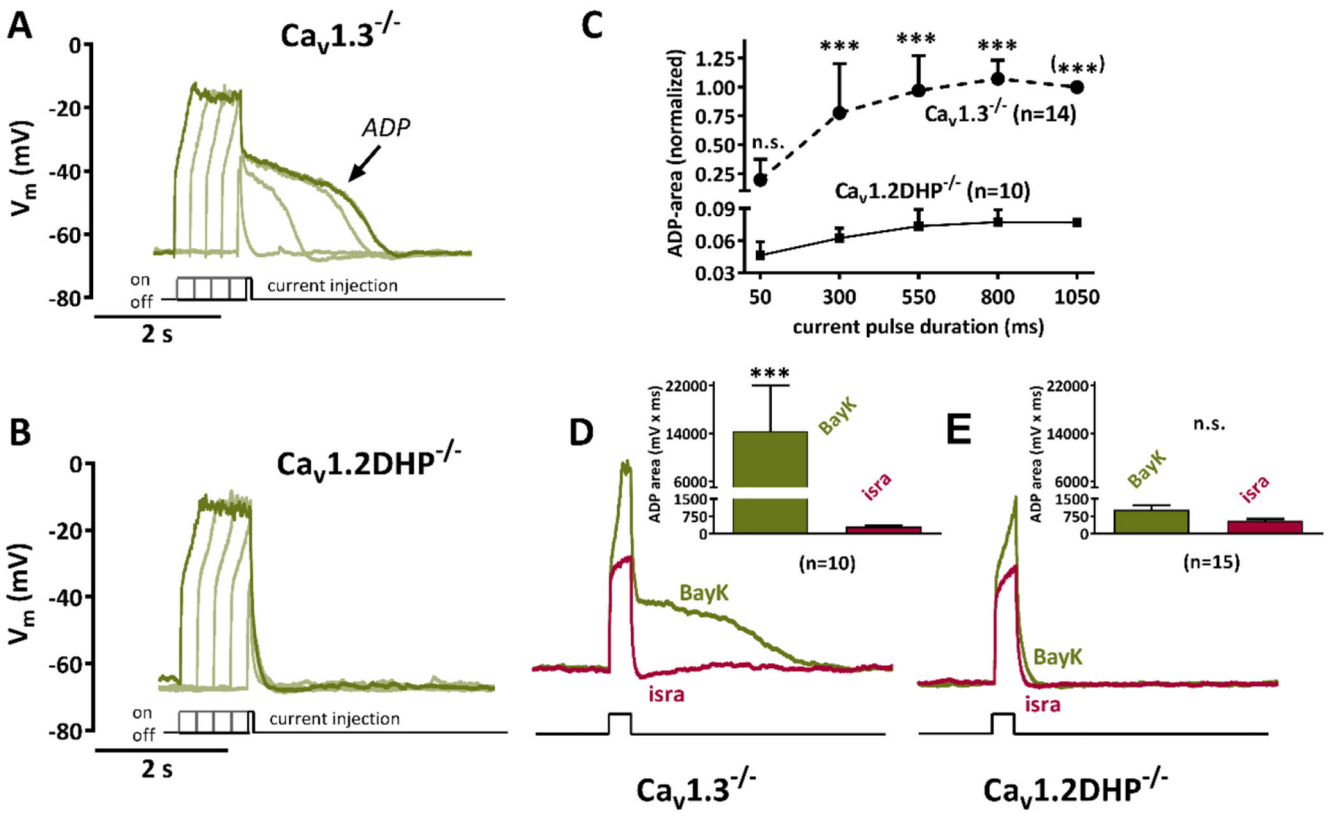

Figure 4. Potentiation of $Ca_V1.2$ but not $Ca_V1.3$ channels gives rise to pronounced afterdepolarizations.

A, **B** Voltage response to brief current injections (50 to 1050 ms duration, increased in 4 steps of 250 ms) that cause depolarizations up to -20 mV in 0.5 μM tetrodotoxin-silenced neurons are shown together with their afterpotentials upon LTCC channel potentiation with 3 μM BayK. Distinct afterdepolarizations (ADP) can be seen in $Ca_V1.3^{-/-}$ neurons (A) but not in $Ca_V1.2DHP^{-/-}$ neurons (B). **C** Summary graph of experiments such as the one illustrated by original traces in A and B for ADP areas of 14 $Ca_V1.3^{-/-}$ neurons and of 10 $Ca_V1.2DHP^{-/-}$ neurons. Data (shown as mean + standard deviation) were normalized to the ADP area at 1050 ms current-injection duration, which is set to 1 for $Ca_V1.3^{-/-}$ neurons and 0.077 for $Ca_V1.2DHP^{-/-}$ neurons, which corresponds to the mean ADP area at this current-injection duration in relation to the mean ADP area of $Ca_V1.3^{-/-}$ neurons. n.s., not significant. (***) indicates that the statistical test had to be been done on the raw data rather than the normalized one for this data point. **D**, **E** Overlay of voltage responses to similar current injections in the presence of BayK and isradipine of $Ca_V1.3^{-/-}$ neurons and of $Ca_V1.2DHP^{-/-}$ neurons. Afterpotentials are blocked by 3 μM isradipine. Note that the y-axis shown in B also applies for the traces in D and E. The graphs in the inserts compare the maximum ADP areas (shown as mean + SEM) that were elicited in the presence of BayK or isradipine (isra) of $Ca_V1.3^{-/-}$ neurons (D, n= 10) and of $Ca_V1.2DHP^{-/-}$ neurons (E, n=15). n.s., not significant.

Europe PMC Funders Author Manuscripts

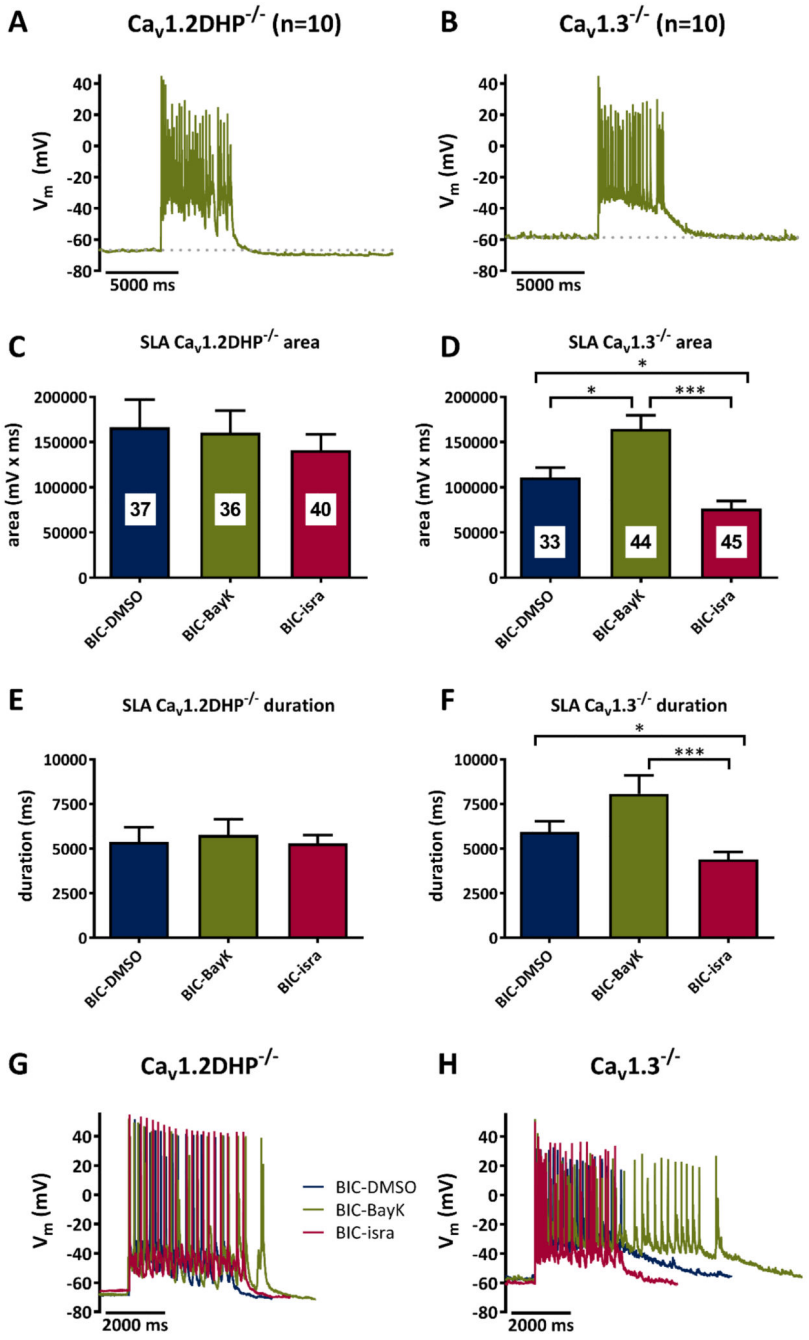

Figure 5. Implication of Ca$_v$1.2 and Ca$_v$1.3 channels in seizure-like activity.

A, **B** Examples of seizure-like activity (SLA) induced by co-application of bicuculline (10 μM) and BayK (3 μM) in Ca$_v$1.2DHP$^{-/-}$ neurons (A) or Ca$_v$1.3$^{-/-}$ neurons (B). **C-F** Analysis of the area (C, D) and duration (E, F) of SLA induced by 10 μM bicuculline in Ca$_v$1.2DHP$^{-/-}$ neurons (C, E) or Ca$_v$1.3-/- neurons (D, F) under three conditions of LTCC activity: endogenous activity (DMSO control), potentiated (BayK, 3 μM) and inhibited (isradipine, 3 μM). The figures in the bars indicate the total number of events evaluated. All statistically significant differences are indicated by horizontal brackets. **G**, **H** Overlay of typical SLA

recorded from $Ca_v1.2DHP^{-/-}$ neurons (G) or $Ca_v1.3^{-/-}$ neurons (H) from the experiments analysed in C to F.

Europe PMC Funders Author Manuscripts

Table 1
Summary of event (PDS, SLA)-area and -duration

B I C – P D S	$Ca_v1.2DHP^{-/-}$ (n=17)			$Ca_v1.3^{-/-}$ (n=18)		
area (mV x ms)	**DMSO**	**BayK**	**isra**	**DMSO**	**BayK**	**isra**
mean	2738	3704	2191	2632	2728	2626
SEM	± 60	± 176	± 50	± 50	± 45	± 52
duration (ms)	**DMSO**	**BayK**	**isra**	**DMSO**	**BayK**	**isra**
mean	135.4	178.3	122.3	125.1	130.1	129.3
SEM	± 2.4	± 5.7	± 2.4	± 1.8	± 1.7	± 2.1

C a f f - P D S	$Ca_v1.2DHP^{-/-}$ (n=11)			$Ca_v1.3^{-/-}$ (n=12)		
area (mV x ms)	**DMSO**	**BayK**	**isra**	**DMSO**	**BayK**	**isra**
mean	1282	2007	1564	805	1141	549
SEM	± 55	± 66	± 72	± 22	± 27	±14
duration (ms)	**DMSO**	**BayK**	**isra**	**DMSO**	**BayK**	**isra**
mean	73.3	101.1	95.8	46.8	62.3	34.0
SEM	± 2.8	± 2.7	± 3.7	± 1.5	± 1.6	± 1.1

B I C - S L A	$Ca_v1.2DHP^{-/-}$ (n=10)			$Ca_v1.3^{-/-}$ (n=10)		
area (mV x ms)	**DMSO**	**BayK**	**isra**	**DMSO**	**BayK**	**isra**
mean	166321	160348	141143	110878	164452	76594
SEM	± 30691	± 24451	± 17252	± 10659	± 15204	± 8168
duration (ms)	**DMSO**	**BayK**	**isra**	**DMSO**	**BayK**	**isra**
mean	5385	5761	5285	5940	8073	4385
SEM	± 799	± 881	± 478	± 595	± 1033	± 416

BayK: 3 μM Bay K8644; BIC: 10 μM bicuculline; Caff: 1 mM caffeine; DMSO: 0.3% dimethyl sulfoxide; isra: 3 μM isradipine; PDS: paroxysmal depolarization shift, SEM: standard error of the mean; SLA: seizure like activity.